

# Majorana Multiplexing

Yang Peng<sup>1,2,\*</sup> and Gil Refael<sup>1</sup>

<sup>1</sup>*Institute of Quantum Information and Matter and Department of Physics,  
California Institute of Technology, Pasadena, CA 91125, USA*

<sup>2</sup>*Walter Burke Institute for Theoretical Physics, California Institute of Technology, Pasadena, CA 91125, USA*

Time-quasiperiodic Majoranas are generalizations of Floquet Majoranas in time-quasiperiodic superconducting systems. We show that in a system driven at  $d$  mutually irrational frequencies, there are up to  $2^d$  types of such Majoranas, coexisting despite spatial overlap and lack of time-translational invariance. Although the quasienergy spectrum is dense in such systems, the time-quasiperiodic Majoranas can be stable and robust against resonances due to localization in the periodic-drives induced synthetic dimensions. This is demonstrated in a time-quasiperiodic Kitaev chain driven at two frequencies. We further relate the existence of multiple Majoranas in a time-quasiperiodic system to the time quasicrystal phase introduced recently. These time-quasiperiodic Majoranas open a new possibility for braiding which will be pursued in the future.

*Introduction.*— Majorana bound states, aka Majoranas, are zero-energy excitations in topological superconductors invariant under particle-hole transformation [1–3]. Their zero-energy nature gives rise to degenerate ground states, which can be used as nonlocal qubits and memory [4–6]. Therefore, Majorana engineering in a variety of platforms has been an simmering field of study both theoretically [7–16] and experimentally [17–28].

Topological phases, however, also exist under nonequilibrium conditions and can be realized by time-periodic driving, known as Floquet engineering. Floquet topological superconductors and superfluids were proposed to be realized in either periodically driven cold atom systems [13, 29] or proximitized nanowires [30, 31]. On the experimental side, various of Floquet topological phases have been realized in the laboratory [32–36].

As it turns out, Floquet topological superconductors (or superfluids) host a dynamical version of Majoranas, dubbed Floquet Majoranas [13, 37]. Rather than sitting at zero energy, Floquet Majoranas have quasienergies  $\epsilon = 0$  or  $\epsilon = \omega/2$ , where  $\omega$  is the driving frequency. Because energy is only defined modulo  $\omega$ ,  $\omega/2$  is a particle-hole symmetric point in the spectrum just as  $\epsilon = 0$  is, and the particle-hole symmetric nature of these Majoranas holds in a time-dependent fashion at all times. Indeed, Floquet Majoranas can form topological qubits and store quantum information, just as their equilibrium counterparts do [37]. Floquet Majoranas may therefore open a new route for topological quantum computation using the time domain as a resource [38].

A natural question arises: could we obtain even more Majoranas with drives at multiple frequencies? This would be similar to frequency multiplexing to enhance the hardware channel capacity in optical fibers [39]. For concreteness, let us consider a time-quasiperiodic superconductor driven at two frequencies  $\omega_1$  and  $\omega_2$ , where  $\omega_1/\omega_2$  is an irrational number, otherwise the system is time-periodic. We assume the concept of quasienergy (as we will introduce it later) also exist in this context, which is defined up to  $n_1\omega_1 + n_2\omega_2$  with  $n_1, n_2 \in \mathbb{Z}$ . Thus, there

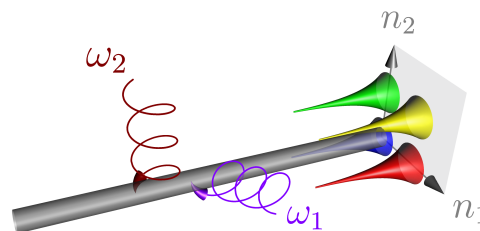


Figure 1. Schematic representation of time-quasiperiodic Majoranas localized at the end of a 1D topological superconductor (in grey) driven at two frequencies  $\omega_1$  and  $\omega_2$ . These Majoranas are localized in both real space and the two synthetic dimensions with coordinates  $n_1$  and  $n_2$ .

are four inequivalent particle-hole symmetric quasienergies:  $0$ ,  $\omega_1/2$ ,  $\omega_2/2$ , and  $(\omega_1 + \omega_2)/2$ . This means one can at most have four types of Majoranas, as shown in Fig. 1. On the other hand, from a naive point of view, since  $n_1\omega_1 + n_2\omega_2$  could be made to yield arbitrary energy increments, as long as  $|n_1|, |n_2|$  are large enough, the quasienergy spectrum will be everywhere dense, with multi-photon energy arbitrarily small near resonances, and these Majoranas appear fully unstable.

In this manuscript, we demonstrate that Majoranas can actually be stable. This is the result of localizations in the drive-induced synthetic  $n_1$  and  $n_2$  dimensions. We confirm this by simulating a Kitaev chain driven at two incommensurate frequencies, and show the existence of Majoranas with half-frequency quasienergies. Furthermore, we use our simulations to demonstrate that time-quasiperiodic Majoranas are related to the “time quasicrystal” phases introduced recently in time-quasiperiodic spin chains [40] (see also Refs. [41–45]); the half-frequency Majoranas are essentially the single-particle degrees of freedom characterizing the time-quasicrystal phase, in the same vein that the Floquet Majoranas are underlying the time-crystal period doubling of Refs. [46–48].

*Floquet recap*— Let us start by briefly reviewing Floquet states. Consider a time-periodic Hamiltonian

$H(t) = H(t + T)$ , with driving angular frequency  $\omega$ , and period  $T = 2\pi/\omega$ . The solutions to the time-dependent Schrödinger equation are characterized by the Floquet states, given by  $|\Psi_\alpha(t)\rangle = e^{-i\epsilon_\alpha t} |\Phi_\alpha(t)\rangle$ , where  $|\Phi_\alpha(t)\rangle$  is a periodic function with the same period as the Hamiltonian, which satisfies the eigenvalue equation  $[H(t) - i\partial_t] |\Phi_\alpha(t)\rangle = \epsilon_\alpha |\Phi_\alpha(t)\rangle$  with eigenvalue  $\epsilon_\alpha$ . Here,  $K(t) = H(t) - i\partial_t$  and  $\epsilon_\alpha$  are called quasienergy operator and quasienergy, respectively.

It is important to note that quasienergies are not uniquely defined. Indeed,  $\epsilon_\alpha$  and  $\epsilon_{\alpha,n} = \epsilon_\alpha + n\omega$  with  $n \in \mathbb{Z}$  actually describe the same physical state  $|\Psi_\alpha(t)\rangle = e^{-i\epsilon_\alpha t} |\Phi_\alpha(t)\rangle = e^{-i\epsilon_{\alpha,n} t} |\Phi_{\alpha,n}(t)\rangle$ , where  $|\Phi_{\alpha,n}(t)\rangle = e^{in\omega t} |\Phi_\alpha(t)\rangle$  is also an eigenfunction of the quasienergy operator at quasienergy  $\epsilon_{\alpha,n}$ . Thus, the quasienergy  $\epsilon_\alpha$  is only uniquely defined modulo  $\omega$ , e.g., in the range  $-\omega/2 \leq \epsilon < \omega/2$ .

*Floquet synthetic dimensions and Wannier-Stark localization*— Our construction of time-quasiperiodic Majoranas requires recasting the driven Hamiltonian in a time-independent way. Let us write out the Hamiltonian and Floquet states using their Fourier expansion of  $H(t) = \sum_n e^{-im\omega t} h_n$  and  $|\Phi_\alpha(t)\rangle = \sum_m e^{-im\omega t} \phi_m^\alpha$ . The eigenvalue equation for the quasienergies then becomes

$$\sum_m h_{n-m} \phi_m^\alpha - n\omega \phi_n^\alpha = \epsilon_\alpha \phi_n^\alpha, \quad (1)$$

which describes particles hopping in a 1D synthetic lattice, spanned by the coordinate  $n$ , with  $\omega$  playing the role of a uniform force field. This is precisely the Hamiltonian for a Wannier-Stark ladder, with energy difference  $\omega$  between neighboring rungs. We will restrict ourselves to nearest-neighbor-hopping models, i.e.  $h_n = 0$  for  $|n| \geq 2$ .

It has been known that the electronic wave functions in the Wannier-Stark ladder are localized, with a localization length  $\sim 1/\ln(\omega/V)$  when  $V < \omega$ , with  $V$  being the nearest neighbor hopping amplitude, known as the Wannier-Stark localization [49, 50]. Likewise we expect that the Floquet states will be localized to the vicinity of a particular  $n$ , which is a manifestation of energy conservation.

*Floquet Particle-hole symmetry in superconductors.* The hamiltonians of superconductors possess a unitary matrix  $U_P$  such that  $U_P H(t)^* = -H(t) U_P$  for all times, with “\*” denoting complex conjugation. This particle-hole symmetry dictates that  $U_P K(t)^* U_P^\dagger = -K(t)$ , and that the Floquet states appear in pairs as  $|\Phi_\alpha(t)\rangle$  and  $U_P |\Phi_\alpha(t)^*\rangle$ , with quasienergies  $\pm\epsilon_\alpha$ , respectively.

Majoranas are special states that are particle-hole symmetric. Namely, with  $|\psi(t)\rangle$  a Majorana state:

$$e^{-i\epsilon t} |\phi(t)\rangle = |\psi(t)\rangle = U_P |\psi(t)^*\rangle = e^{i\epsilon t} U_P |\phi(t)^*\rangle, \quad (2)$$

which works if  $(U_P |\phi(t)^*\rangle) = e^{-ip\omega} |\phi(t)\rangle = e^{-2i\epsilon t} |\phi(t)\rangle$  with some  $p \in \mathbb{Z}$ . Therefore, the majorana quasienergies are restricted to  $\epsilon = p\omega/2$  with some  $p \in \mathbb{Z}$ . And because

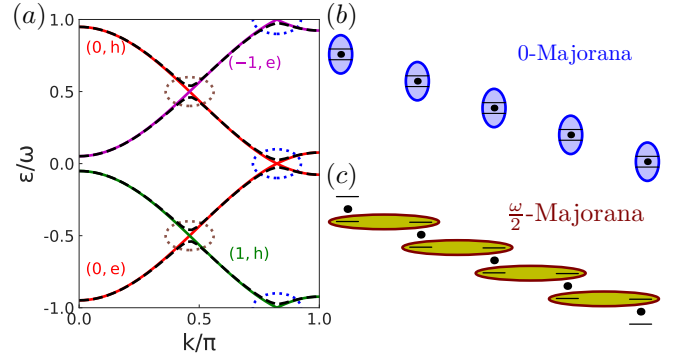


Figure 2. (a) Quasienergy spectrum as a function of  $k$  between  $-\omega$  and  $\omega$ , for the model defined in Eqs. (3,4). The black dashed lines are obtained with  $J = 2$ ,  $\mu = 3.4$ ,  $\omega = 3.9$ ,  $\Delta = 0.2$ , and  $\Delta' = 0.15$ . The solid red, green, and magenta lines corresponding to the quasienergies  $\epsilon_{n,e/h}$  when setting  $\Delta = \Delta' = 0$ , for a certain  $(n, e/h)$ , as indicated in the figure with the same color. The two types of topological gaps are indicated in the blue and brown dotted circles. (b) and (c) are the Wannier-Stark ladders with two orbitals (black lines) per rung (black dot), when  $\epsilon_{n,e} \simeq \epsilon_{n,h}$  and  $\epsilon_{n+1,h} \simeq \epsilon_{n,e}$  respectively. The 0-Majoranas are formed from equal superposition between states  $(n, e)$  and  $(n, h)$  (blue ellipses), while the  $\omega/2$ -Majoranas are formed from equal superposition between states  $(n + 1, h)$  and  $(n, e)$  (green ellipses).

shifts by  $\omega$  are just a gauge choice, there are only two inequivalent Floquet Majoranas [13, 37], with  $p \in \{0, 1\}$  reduced to a  $\mathbb{Z}_2$  variable.

*Floquet Majoranas.* Next consider a 1D Floquet topological superconductor, with Hamiltonian  $H(t) = H_K + M(\omega t)$ . The first term describes a static Kitaev chain

$$H_K = -\mu \sum_{j=1}^N c_j^\dagger c_j - \sum_{j=1}^{N-1} [(Jc_j^\dagger c_{j+1} + i\Delta c_j c_{j+1}) + h.c.], \quad (3)$$

with  $c_j$  ( $c_j^\dagger$ ) annihilation (creation) operators at site  $j$ ,  $\mu$  is the chemical potential,  $J$  is the hopping amplitude, and  $\Delta$  is the  $p$ -wave pairing potential. The second term,

$$M(\omega t) = -i\Delta' \sum_{j=1}^{N-1} (e^{-i\omega t} c_j c_{j+1} - e^{i\omega t} c_{j+1}^\dagger c_j^\dagger), \quad (4)$$

corresponds to a periodic drive. Introducing Nambu spinors in momentum ( $k$ ) space  $\Psi_k^\dagger = (c_k^\dagger, c_{-k})$ , with  $c_k = \sum_{j=1}^N c_j e^{-ikj} / \sqrt{N}$ . For periodic boundary conditions, we get the Bogoliubov-de Gennes Hamiltonian

$$H = \sum_{k>0} \Psi_k^\dagger [\mathcal{H}_K(k) + \mathcal{M}(k, \omega t)] \Psi(k), \quad (5)$$

$$\mathcal{H}_K(k) = \tau_z \xi_k + \tau_x \Delta \sin k, \quad \mathcal{M}(k, \omega t) = \tau_x \Delta' \sin k e^{i\omega t \tau_z}$$

where  $\tau_{x,y,z}$  are the Pauli matrices in Nambu space, and  $\xi_k = -J \cos k - \mu/2$  is the normal state dispersion.

Considering the driven Kitaev model using the synthetic dimension and Wannier-Stark-ladder approach of

Eq. (1), we can interpret the model's spectrum as follows. For each  $k$  there are two orbitals for each harmonic  $n$ . Thus, in the absence of pairing potential, the system has two groups of equally spaced spectra  $\epsilon_{n,e/h} = \pm\xi_k + n\omega$ , with  $n \in \mathbb{Z}$ . The + or - signs indicate electron-like (e) or hole-like (h) states. The static pairing potential  $\Delta$  opens a topological gap at  $n\omega$ , when  $\epsilon_{n,e} = \epsilon_{n,h}$ , while the dynamical pairing  $\Delta'$  opens a topological gap at  $(n+1)\omega/2$  when  $\epsilon_{n+1,h} = \epsilon_{n,e}$ , i.e., at the edge of the 'Floquet zone'. In Fig. 2(a), we show the spectrum of the ladder as a function of  $k$  in a window between  $-\omega$  and  $\omega$ , with a set of parameters producing the two topological gaps. In an open chain, these gaps produce the two types of Floquet Majoranas at quasienergies 0 and  $\omega/2$ , created with equal superposition of electron- and hole-like states within the same rung (see Fig. 2(b)), and between neighboring rungs (see Fig. 2(c)), respectively.

*Time-quasiperiodic Majoranas.*— Our main result is that Majoranas also emerge due to multi-frequency drive. Consider a time-quasiperiodic Hamiltonian  $H(t)$  characterized by  $d$  mutually irrational frequencies  $\boldsymbol{\omega} = (\omega_1, \dots, \omega_d)$ . It turns out that the Floquet ansatz introduced previously can be trivially generalized to the time-quasiperiodic system [51]. The function  $|\Phi_\alpha(t)\rangle$ , which becomes time-quasiperiodic at frequencies specified by  $\boldsymbol{\omega}$ , satisfies the eigenvalue equation of the time-quasiperiodic quasienergy operator  $K(t)$ :

$$K(t)|\Phi_\alpha(t)\rangle = \left( H(t) - i\frac{\partial}{\partial t} \right) |\Phi_\alpha(t)\rangle = \epsilon_\alpha |\Phi_\alpha(t)\rangle \quad (6)$$

with the quasienergy  $\epsilon_\alpha$  defined modulo  $\mathbf{n} \cdot \boldsymbol{\omega}$ .

Time-quasiperiodic Majoranas then emerge as particle-hole symmetric states. These must have quasienergies  $\epsilon = \mathbf{p} \cdot \boldsymbol{\omega}/2$ , with  $\mathbf{p} \in \mathbb{Z}^d$ . Furthermore, they fall into  $2^d$  groups, reducing  $\mathbf{p} \in \{0, 1\}^d$ , corresponding to  $2^d$  types of Majoranas.

Contrary to a gapped Floquet topological phase, the quasienergy spectra in a time-quasiperiodic system are dense, since  $\mathbf{n} \cdot \boldsymbol{\omega}$  can approach any value. It seems, therefore, that time-quasiperiodic Majoranas do not have a gap that could protect them from hybridizing with bulk states due to local perturbations. In what follows, however, we show that these majoranas are stable not due to a gap, but rather due to localization in the drive-induced synthetic dimensions.

*Multidrive synthetic Lattice and localization*— Similar to the Floquet case, one can also look at the time-quasiperiodic system from a time-independent perspective. The quasienergy eigenvalue equation becomes a tight-binding problem on a  $d$ -dimensional lattice whose coordinates are given by  $\mathbf{n} \in \mathbb{Z}^d$  embedded in the  $d$ -dimensional Euclidean space  $\mathbb{R}^d$ . In addition, a force field given by  $\boldsymbol{\omega}$  pointing into the synthetic dimensions keeps track of the energy of energy quanta absorbed from the drive [52, 53].

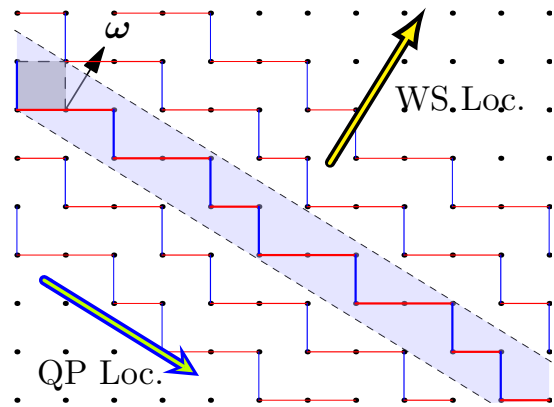


Figure 3. 2D synthetic lattice with an electric field  $\boldsymbol{\omega} = (\omega_1, \omega_2)$ . The equipotential lines perpendicular to  $\boldsymbol{\omega}$  are denoted as black dashed lines. One obtains a 1D quasicrystal in between the two dashed lines denoted as the blue region. The nearest-neighbor couplings within the quasicrystal are denoted as solid red or blue lines, corresponding to the original horizontal and vertical couplings. The two big arrows denotes the directions along which there are localizations: Wannier-Stark (WS) vs. Quasiperiodic (QP).

The equipotential surface perpendicular to the synthetic electric field defines a  $(d-1)$ -dimensional quasicrystal [54]. Fig. 3 describes the quasicrystal construction for  $d=2$ , which is easily generalized to more dimensions. The lattice sites in a narrow strip (contained in the blue region) normal to the frequency vector  $\boldsymbol{\omega}$  make a one-dimensional (1D) quasicrystal where the on-site energy goes up and down by  $\omega_2$  and  $\omega_1$ . By shifting the strip along  $\boldsymbol{\omega}$ , the whole two-dimensional (2D) lattice will be covered, and every lattice sites will be uniquely contained in one 1D quasicrystal. Hence, the original system is equivalent to a Wannier-Stark ladder of 1D quasicrystals.

Now it is clear, however, what can protect majoranas from bulk hybridization. Motion in a quasicrystal is fully localized if the hopping strength is smaller than the quasiperiodic modulation of the on-site potential [55, 56].

Therefore, Majoranas can emerge due to combining three different localization mechanisms: 1) real space localization due to the superconducting gap; 2) Wannier-Stark localization along the direction of the 'electric' field; 3) Quasiperiodic localization within the quasicrystal spanned perpendicular to the field. We focus on the time-quasiperiodic Kitaev chain  $H(t) = H_K + M(\omega_1 t) + M(\omega_2 t)$ , following Eqs. (3, 4), with  $\frac{\omega_2}{\omega_1} = \frac{\sqrt{5}+1}{2}$ . When considering this system in the synthetic space  $n_1, n_2$  of harmonics of the  $\omega_1, \omega_2$  drives, the system is localized along the  $\boldsymbol{\omega}$  direction due to Wannier-Stark localization. The system is localized perpendicular to  $\boldsymbol{\omega}$  due to quasiperiodic localization when  $\Delta' < \omega_1, \omega_2$ . On a ring, there are two orbitals per rung for each quasimomentum  $k$ . Ignoring the pairing potentials  $\Delta, \Delta'$ , the eigenval-

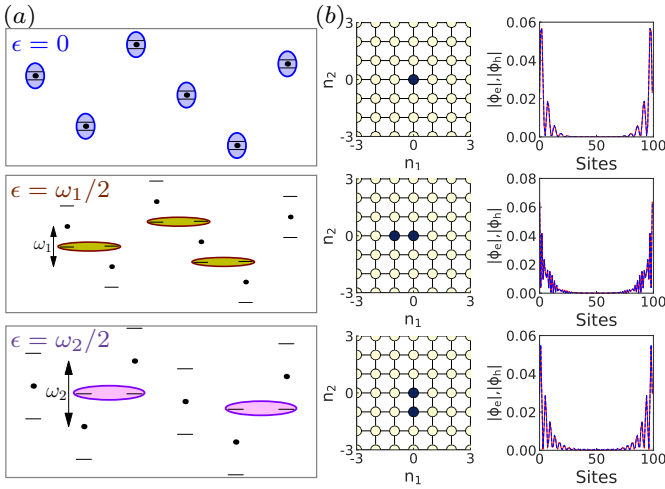


Figure 4. (a) The quasiperiodic ladder perpendicular to  $\omega$  in the 2D synthetic lattice, with each rung corresponding to a Kitaev chain. For a periodic chain, when  $k$  is close to three special quasimomenta such that  $\epsilon_{n_1, n_2, e} \simeq \epsilon_{n_1, n_2, h}$  (top),  $\epsilon_{n_1+1, n_2, h} \simeq \epsilon_{n_1, n_2, e}$  (middle), and  $\epsilon_{n_1, n_2+1, h} \simeq \epsilon_{n_1, n_2, e}$  (bottom), topological gaps are induced. The three types of topological gaps give rise to three types of Majoranas in an open chain. (b) Numerical solution of the 0-frequency and time-quasiperiodic Majorana states on the 2D synthetic lattice of size  $15 \times 15$ . Each site of the lattice corresponding to a Kitaev chain of length  $N = 100$ . Left:  $|\phi_{n_1, n_2}|^2$  for the 0,  $\frac{\omega_1}{2}$ , and  $\frac{\omega_2}{2}$  Majoranas on the 2D synthetic lattice, where the darker color corresponds to a larger magnitude. Right: the absolute value of the corresponding Majorana wave function, summed over the 2D synthetic lattice. The electron and hole components  $\phi_e, \phi_h$  are plotted as red solid and blue dashed curves. The other parameters are  $\omega_1 = 3.9$ ,  $\omega_2 = \omega_1 \times (\sqrt{5} + 1)/2$ ,  $J = 2$ ,  $\mu = 3.4$ ,  $\Delta = 0.2$ , and  $\Delta' = 0.15$ .

ues of this system are  $\epsilon_{n_1, n_2, e/h} = \pm \xi_k + n_1 \omega_1 + n_2 \omega_2$ . By choosing proper parameters, one has three special quasimomenta at which  $\epsilon_{n_1, n_2, e} = \epsilon_{n_1, n_2, h}$ ,  $\epsilon_{n_1+1, n_2, h} = \epsilon_{n_1, n_2, e}$ , and  $\epsilon_{n_1, n_2+1, h} = \epsilon_{n_1, n_2, e}$ .  $\Delta$  and  $\Delta'$ , however, open topological gaps at these crossings. In an open chain, these gaps give rise to three kinds of Majoranas, with quasienergies 0,  $\omega_1/2$  and  $\omega_2/2$  (Fig. 4(a)). The existence, stability, and localization of these Majoranas are verified via numerical simulation outlined in the supplemental material [51]. Fig. 4(b) shows these wavefunctions  $\phi_{n_1, n_2} = (\phi_{n_1, n_2, e}, \phi_{n_1, n_2, h})$  in the synthetic and real spaces. Indeed, the wavefunction, which is identical for the hole and electron components, is localized at a single, or two neighboring sites, in the synthetic directions, and near the edges in real space.

*From Majorana multiplexing to time quasicrystal.*— The different types of Majoranas, gives rise to a quasiperiodic oscillating pattern distinct from the driving pattern in the correlation function  $\langle \hat{O}(t) \hat{O}(0) \rangle$  of a local observable  $\hat{O}$ , resembling the time quasicrystal of Ref. [40]. Take, for instance,  $\hat{O}$  to be  $\gamma_1 = (c_1 + c_1^\dagger)/\sqrt{2}$ , with  $c_1, c_1^\dagger$  the electron creation and annihilation oper-

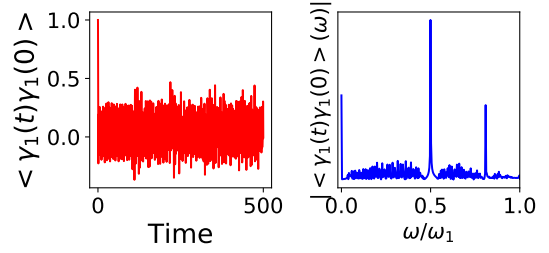


Figure 5. Left: Time evolution of  $\langle \gamma_1(t) \gamma_1(0) \rangle$  simulated on the time-quasiperiodic Kitaev chain, with the same parameters as in Fig. 4. Right: The Fourier transform of  $\langle \gamma_1(t) \gamma_1(0) \rangle$  in the frequency domain. There are three dominant peaks at 0,  $\omega_1/2$ , and  $\omega_2/2 \simeq 0.81\omega_1$ .

ators at the first site. The correlation function is then closely related to the local spectral function, and is dominated by the boundary modes, namely, the Majorana operators

$$\gamma_1(t) = c_0 \psi_0(t) + c_1 \psi_1(t) + c_2 \psi_2(t) + \dots \quad (7)$$

where  $\psi_{0,1,2}$  are the time-quasiperiodic Majorana operators at quasienergies 0,  $\omega_1/2$  and  $\omega_2/2$ . Hence,  $\langle \gamma_1(t) \gamma_1(0) \rangle$  generically contains peaks at frequencies, 0,  $\omega_1/2$  and  $\omega_2/2$  (see Fig. 5), where the average is with respect to the BCS vacuum at  $t = 0$ . In fact, the spectral peaks at half-frequencies persist even we include temporal disorders or take commensurate frequencies (see the Supp. Mat. Ref. [51] for details).

If one applies a Jordan-Wigner transform of the time-quasiperiodic Kitaev chain, we get a time-quasiperiodic Heisenberg model.  $\langle \gamma_1(t) \gamma_1(0) \rangle$  becomes the spin correlation function  $\langle \sigma_1^x(t) \sigma_1(0) \rangle$ . This shows that the time-quasiperiodic Majoranas in a fermionic system are indeed the single-particle degrees of freedom which are responsible for the formation of the time quasicrystal correlations discussed in Ref. [40].

*Conclusion.* — In this work, we generalize the concept of Floquet Majoranas to a time-quasiperiodic system. We show that there are at most  $2^d$  types of Majoranas at quasienergies  $\mathbf{p} \cdot \boldsymbol{\omega}/2$ , with  $\mathbf{p} \in \{0, 1\}^d$  with  $\boldsymbol{\omega} = (\omega_1, \dots, \omega_d)$  consisting of  $d$  mutually irrational frequencies. We study a particular time-quasiperiodic Kitaev chain with  $d = 2$ , and found stable and robust Majoranas at quasienergies 0,  $\omega_1/2$  and  $\omega_2/2$  coexist. The localization in synthetic dimensions, emerges as a resource that allows these Majoranas despite a dense quasienergy spectrum. These Majoranas are also the single-particle degrees of freedom which are relevant to the formation of time quasicrystal [40].

The existence of time-quasiperiodic Majoranas opens a new direction for performing and controlling topological quantum computation using the time domain as a resource for topological ancilla qubits, for instance. Instead of using multiple static topological superconduct-

ing wires, one can dynamically generate multiple Majoranas at different locations for manipulation, by driving a single superconductor at different frequencies in different regions. While this raises issues of equilibration and heating, protocols for finite time manipulation may keep such problems at bay, even if these may be experimentally challenging at present. We intend to investigate these directions in our future research.

*Acknowledgments.*—We acknowledge support from the IQIM, an NSF physics frontier center funded in part by the Moore Foundation. Y. P. is grateful to support from the Walter Burke Institute for Theoretical Physics at Caltech. G. R. is grateful to support from the ARO MURI W911NF-16-1-0361 “Quantum Materials by Design with Electromagnetic Excitation” sponsored by the U.S. Army.

---

\* yangpeng@caltech.edu

- [1] A. Kitaev, *Phys. Usp.* **44**, 131 (2001).
- [2] J. Alicea, Reports on progress in physics **75**, 076501 (2012).
- [3] C. Beenakker, (2013).
- [4] A. Y. Kitaev, *Ann. Phys.* **303**, 2 (2003).
- [5] C. Nayak, S. H. Simon, A. Stern, M. Freedman, and S. Das Sarma, *Rev. Mod. Phys.* **80**, 1083 (2008).
- [6] D. Aasen, M. Hell, R. V. Mishmash, A. Higginbotham, J. Danon, M. Leijnse, T. S. Jespersen, J. A. Folk, C. M. Marcus, K. Flensberg, and J. Alicea, *Phys. Rev. X* **6**, 031016 (2016).
- [7] L. Fu and C. L. Kane, *Phys. Rev. Lett.* **100**, 096407 (2008).
- [8] C. Zhang, S. Tewari, R. M. Lutchyn, and S. Das Sarma, *Phys. Rev. Lett.* **101**, 160401 (2008).
- [9] M. Sato, Y. Takahashi, and S. Fujimoto, *Phys. Rev. Lett.* **103**, 020401 (2009).
- [10] R. M. Lutchyn, J. D. Sau, and S. Das Sarma, *Phys. Rev. Lett.* **105**, 077001 (2010).
- [11] Y. Oreg, G. Refael, and F. von Oppen, *Phys. Rev. Lett.* **105**, 177002 (2010).
- [12] S. Diehl, E. Rico, M. A. Baranov, and P. Zoller, *Nature Physics* **7**, 971 (2011).
- [13] L. Jiang, T. Kitagawa, J. Alicea, A. R. Akhmerov, D. Pekker, G. Refael, J. I. Cirac, E. Demler, M. D. Lukin, and P. Zoller, *Phys. Rev. Lett.* **106**, 220402 (2011).
- [14] S. Nadj-Perge, I. K. Drozdov, B. A. Bernevig, and A. Yazdani, *Phys. Rev. B* **88**, 020407 (2013).
- [15] F. Pientka, L. I. Glazman, and F. von Oppen, *Phys. Rev. B* **88**, 155420 (2013).
- [16] Y. Peng, F. Pientka, L. I. Glazman, and F. von Oppen, *Phys. Rev. Lett.* **114**, 106801 (2015).
- [17] V. Mourik, K. Zuo, S. M. Frolov, S. Plissard, E. P. Bakkers, and L. P. Kouwenhoven, *Science* **336**, 1003 (2012).
- [18] A. Das, Y. Ronen, Y. Most, Y. Oreg, M. Heiblum, and H. Shtrikman, *Nature Physics* **8**, 887 (2012).
- [19] H. O. H. Churchill, V. Fatemi, K. Grove-Rasmussen, M. T. Deng, P. Caroff, H. Q. Xu, and C. M. Marcus, *Phys. Rev. B* **87**, 241401 (2013).
- [20] M. Deng, C. Yu, G. Huang, M. Larsson, P. Caroff, and H. Xu, *Nano letters* **12**, 6414 (2012).
- [21] A. Finck, D. Van Harlingen, P. Mohseni, K. Jung, and X. Li, *Physical review letters* **110**, 126406 (2013).
- [22] S. Nadj-Perge, I. K. Drozdov, J. Li, H. Chen, S. Jeon, J. Seo, A. H. MacDonald, B. A. Bernevig, and A. Yazdani, *Science* **346**, 602 (2014).
- [23] M. Ruby, F. Pientka, Y. Peng, F. von Oppen, B. W. Heinrich, and K. J. Franke, *Phys. Rev. Lett.* **115**, 197204 (2015).
- [24] R. Pawlak, M. Kisiel, J. Klinovaja, T. Meier, S. Kawai, T. Glatzel, D. Loss, and E. Meyer, *npj Quantum Information* **2**, 16035 (2016).
- [25] M. Deng, S. Vaitiekėnas, E. B. Hansen, J. Danon, M. Leijnse, K. Flensberg, J. Nygård, P. Krogstrup, and C. M. Marcus, *Science* **354**, 1557 (2016).
- [26] S. M. Albrecht, A. Higginbotham, M. Madsen, F. Kuemmeth, T. S. Jespersen, J. Nygård, P. Krogstrup, and C. Marcus, *Nature* **531**, 206 (2016).
- [27] M. Ruby, B. W. Heinrich, Y. Peng, F. von Oppen, and K. J. Franke, *Nano letters* **17**, 4473 (2017).
- [28] Ö. Gül, H. Zhang, J. D. Bommer, M. W. de Moor, D. Car, S. R. Plissard, E. P. Bakkers, A. Geresdi, K. Watanabe, T. Taniguchi, *et al.*, *Nature nanotechnology* , 1 (2018).
- [29] M. S. Foster, V. Gurarie, M. Dzero, and E. A. Yuzbashyan, *Phys. Rev. Lett.* **113**, 076403 (2014).
- [30] J. Klinovaja, P. Stano, and D. Loss, *Phys. Rev. Lett.* **116**, 176401 (2016).
- [31] M. Thakurathi, D. Loss, and J. Klinovaja, *Phys. Rev. B* **95**, 155407 (2017).
- [32] Y. Wang, H. Steinberg, P. Jarillo-Herrero, and N. Gedik, *Science* **342**, 453 (2013).
- [33] G. Jotzu, M. Messer, R. Desbuquois, M. Lebrat, T. Uehlinger, D. Greif, and T. Esslinger, *Nature* **515**, 237 (2014).
- [34] M. Aidelsburger, M. Lohse, C. Schweizer, M. Atala, J. T. Barreiro, S. Nascimbene, N. Cooper, I. Bloch, and N. Goldman, *Nature Physics* **11**, 162 (2015).
- [35] M. Tarnowski, F. N. Ünal, N. Fläschner, B. S. Rem, A. Eckardt, K. Sengstock, and C. Weitenberg, arXiv:1709.01046 (2017).
- [36] L. J. Maczewsky, J. M. Zeuner, S. Nolte, and A. Szameit, *Nature communications* **8**, 13756 (2017).
- [37] D. E. Liu, A. Levchenko, and H. U. Baranger, *Phys. Rev. Lett.* **111**, 047002 (2013).
- [38] T. Karzig, B. Bauer, T. Pereg-Barnea, Y. Oreg, and G. Refael, in preparation.
- [39] W. Tomlinson, *Applied Optics* **16**, 2180 (1977).
- [40] P. T. Dumitrescu, R. Vasseur, and A. C. Potter, *Phys. Rev. Lett.* **120**, 070602 (2018).
- [41] T. Li, Z.-X. Gong, Z.-Q. Yin, H. T. Quan, X. Yin, P. Zhang, L.-M. Duan, and X. Zhang, *Phys. Rev. Lett.* **109**, 163001 (2012).
- [42] F. Flicker, arXiv preprint arXiv:1707.09371 (2017).
- [43] S. Autti, G. Volovik, and V. Etlsov, arXiv preprint arXiv:1712.06877 (2017).
- [44] Y. Huang, T. Li, and Z.-q. Yin, *Phys. Rev. A* **97**, 012115 (2018).
- [45] K. Giergiel, A. Miroszewski, and K. Sacha, *Phys. Rev. Lett.* **120**, 140401 (2018).
- [46] V. Khemani, A. Lazarides, R. Moessner, and S. L. Sondhi, *Phys. Rev. Lett.* **116**, 250401 (2016).
- [47] D. V. Else, B. Bauer, and C. Nayak, *Phys. Rev. Lett.*

- [117, 090402 \(2016\)](#).
- [48] A. C. Potter, T. Morimoto, and A. Vishwanath, *Phys. Rev. X* **6**, 041001 (2016).
- [49] H. Fukuyama, R. A. Bari, and H. C. Fogedby, *Phys. Rev. B* **8**, 5579 (1973).
- [50] D. Emin and C. F. Hart, *Phys. Rev. B* **36**, 7353 (1987).
- [51] Supplemental Material.
- [52] I. Martin, G. Refael, and B. Halperin, *Phys. Rev. X* **7**, 041008 (2017).
- [53] Y. Peng and G. Refael, *Phys. Rev. B* **97**, 134303 (2018).
- [54] M. Duneau and A. Katz, *Phys. Rev. Lett.* **54**, 2688 (1985).
- [55] S. Aubry and G. André, *Ann. Israel Phys. Soc* **3**, 18 (1980).
- [56] Y. Lahini, R. Pugatch, F. Pozzi, M. Sorel, R. Morandotti, N. Davidson, and Y. Silberberg, *Phys. Rev. Lett.* **103**, 013901 (2009).
-

**SUPPLEMENTAL MATERIAL**

**FLOQUET ANSATZ FOR TIME-QUASIPERIODIC SYSTEMS**

In this section, we will prove the validity of Floquet ansatz in a time-quasiperiodic system. Namely, the solution  $\Psi(t)$  to a time-dependent Schrödinger equation in a time-quasiperiodic system can be written as  $\Psi(t) = e^{-i\epsilon t}\Phi(t)$  with quasienergy  $\epsilon$  and time-quasiperiodic  $\Phi(t)$ .

A time-dependent Hamiltonian  $H(t)$  is time-quasiperiodic with  $d$  frequencies if  $H(t) = h(\omega_1 t, \dots, \omega_d t)$ , where  $h(\theta_1, \dots, \theta_d)$  is a function of with  $d$   $2\pi$ -periodic arguments  $\boldsymbol{\theta} = (\theta_1, \dots, \theta_d)$  living on a  $d$ -dimensional torus  $\mathbb{T}^d = (\mathbb{R}/2\pi\mathbb{Z})^d$ . The frequencies  $\boldsymbol{\omega} = (\omega_1, \dots, \omega_d)$  are assumed to be mutually irrational, namely

$$\sum_{j=1}^d n_j \omega_j \neq 0, \quad \forall \mathbf{n} = (n_1, \dots, n_d) \in \mathbb{Z}^d. \quad (1)$$

Consider the time evolution of an arbitrary state  $\Psi(t)$  which obeys the time-dependent Schrödinger equation (SEQ)

$$i\dot{\Psi}(t) = H(t)\Psi(t), \quad \dot{\Psi} = \partial_t \Psi. \quad (2)$$

If we write  $\Psi(t) = \psi(\boldsymbol{\theta})$ , with  $\boldsymbol{\theta} = \boldsymbol{\omega}t$ , the above equation can be rewritten as

$$i\boldsymbol{\omega} \cdot \nabla_{\boldsymbol{\theta}} \psi(\boldsymbol{\theta}) = h(\boldsymbol{\theta})\psi(\boldsymbol{\theta}). \quad (3)$$

Let us formally divide  $\boldsymbol{\theta}$  into two parts as  $\boldsymbol{\theta} = (\boldsymbol{\theta}_{\perp}, \theta_k)$ , where  $\boldsymbol{\theta}_{\perp}$  is a vector consisting of  $\theta_j$ s with  $j = 1, \dots, d, j \neq k$ . Similarly, we write  $\boldsymbol{\omega} = (\boldsymbol{\omega}_{\perp}, \omega_k)$ .

Thus, we obtain a new SEQ

$$i\omega_k \partial_{\theta_k} \psi(\boldsymbol{\theta}_{\perp}, \theta_k) = [h(\boldsymbol{\theta}_{\perp}, \theta_k) - i\boldsymbol{\omega}_{\perp} \cdot \nabla_{\boldsymbol{\theta}_{\perp}}] \psi(\boldsymbol{\theta}_{\perp}, \theta_k). \quad (4)$$

By Floquet theorem, the solutions to this SEQ can be written as

$$\psi(\boldsymbol{\theta}_{\perp}, \theta_k) = \exp(-i\epsilon_k \theta_k / \omega_k) \phi_d(\boldsymbol{\theta}_{\perp}, \theta_k) \quad (5)$$

with  $\phi_k(\boldsymbol{\theta}_{\perp}, \theta_k) = \phi_k(\boldsymbol{\theta}_{\perp}, \theta_k + 2\pi)$ . Hence,  $\psi(\boldsymbol{\theta}) \exp(i\epsilon_k \theta_k / \omega_k)$  is  $2\pi$ -periodic in its  $k$ th argument  $\theta_k$ . Since  $k$  is an arbitrary number from 1 to  $d$ ,

$$\phi(\boldsymbol{\theta}) = \psi(\boldsymbol{\theta}) \exp(i \sum_{j=1}^d \epsilon_j \theta_j / \omega_j) \quad (6)$$

will be  $2\pi$ -periodic in all  $\theta_j$ s with proper chosen  $\epsilon_j$ s.

As a result, a quasiperiodic function  $\Phi(t) = \phi(\boldsymbol{\theta})$  can be constructed by setting  $\boldsymbol{\theta} = \boldsymbol{\omega}t$ . We thus obtain a factorization

$$\Psi(t) = \Phi(t) \exp(-i\epsilon t), \quad \epsilon = \sum_{j=1}^d \epsilon_j, \quad (7)$$

with  $\Phi(t)$  time-quasiperiodic in the same frequencies. Moreover, this function satisfies

$$[H(t) - i\partial_t] \Phi(t) = \epsilon \Phi(t), \quad (8)$$

which is Eq. (6) in the main text.

**WANNIER-STARK LOCALIZATION OF FLOQUET MAJORANAS**

Let us consider the time-periodic Kitaev chain introduced in the main text, with Hamiltonian  $H(t) = H_K + M(\omega t)$ . The static part is

$$H_K = -\mu \sum_{j=1}^N c_j^{\dagger} c_j - \sum_{j=1}^{N-1} [(J c_j^{\dagger} c_{j+1} + i\Delta c_j c_{j+1}) + h.c.], \quad (9)$$



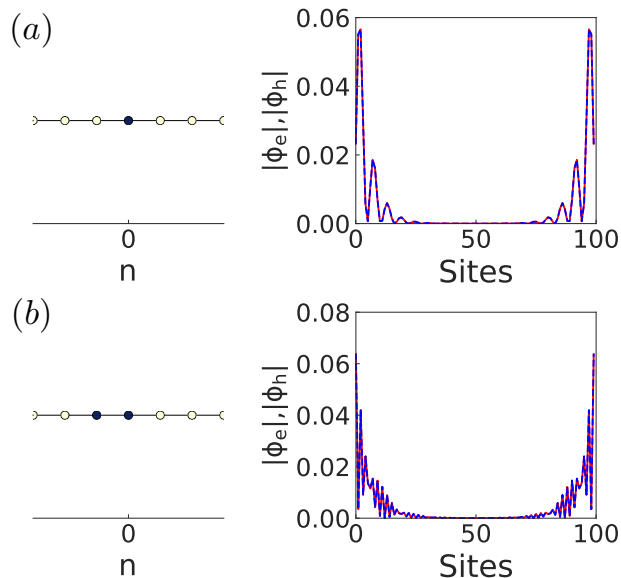


Figure 6. Numerical results for the Floquet Majorana wave functions in a Wannier-Stark ladder of 30 rungs, for a time-periodic Kitaev chain of  $N = 100$  sites. The left panels are the magnitude of  $|\phi_n|$  (summed over electron and hole components), where darker color corresponds to larger magnitude. The right panels are the absolute value of the corresponding Majorana wave function, summed over the 1D synthetic lattice. The electron and hole components  $\phi_e$  and  $\phi_h$  are plotted as red solid and blue dashed curves. (a) and (b) are for Majoranas at quasienergies 0 and  $\omega/2$ , respectively. The other parameters are  $\omega = 3.9$ ,  $J = 2$ ,  $\mu = 3.4$ , and  $\Delta = 0.2$ .

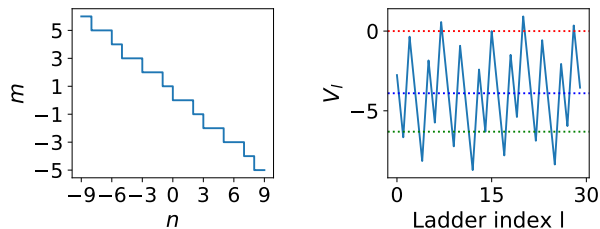


Figure 7. Left: 1D quasiperiodic ladder obtained by cutting the 2D synthetic lattice with equipotential surfaces. Right: Onsite potential  $V_l$  as a function of the ladder index  $l$ . We indicate the energy at 0,  $-\omega_1$ ,  $-\omega_2$  by the red, blue and green dotted lines for reference.

The time-quasiperiodic Kitaev chain introduced in the main text can be mapped to a 2D synthetic lattice with an additional electric field. Perpendicular to the field, we have a quasiperiodic ladder climbing up or down by either  $\omega_1$  or  $\omega_2$  between two rungs, depending on whether these two rungs are connected horizontally or vertically in the original 2D synthetic lattice. In Fig. 7 we show a quasiperiodic ladder of length 30 obtained in a 2D lattice, and its on-site potential  $V_l$  as a function the ladder index  $l$ .

Moreover, the hopping matrix (from the  $n$ th to the  $(n + 1)$ th rung of the ladder) is

$$h_{-1,0} = -\frac{i\Delta'}{2} \begin{pmatrix} 0 & \tau_+ & & & \\ -\tau_+ & 0 & \tau_+ & & \\ & -\tau_+ & \ddots & \ddots & \\ & & \ddots & 0 & \tau_+ \\ & & & -\tau_+ & 0 \end{pmatrix} \quad (16)$$

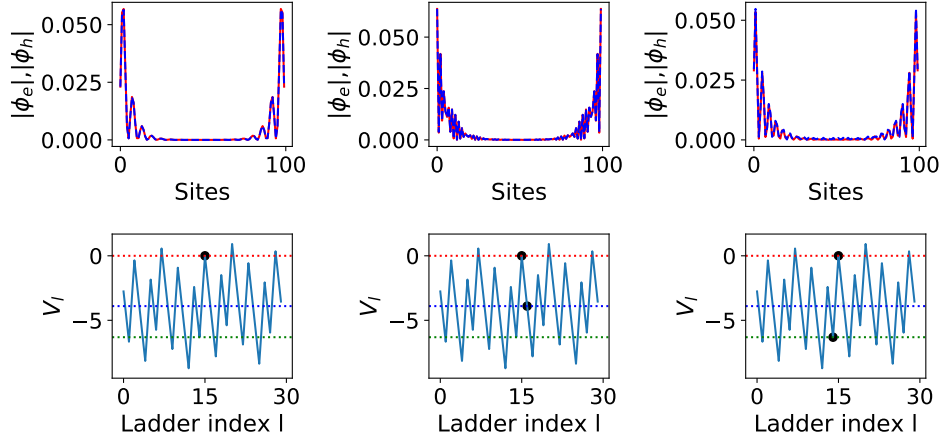


Figure 8. Majorana wave functions in a quasiperiodic ladder of 30 rungs, where each rung contains a Kitaev chain of  $N = 100$  sites. Upper: the absolute value of the Majorana wave function, summed over the quasiperiodic ladder. The electron and hole components  $\phi_e$  and  $\phi_h$  are plotted as red solid and blue dashed curves. Lower: the magnitude of  $|\phi_j|$  (summed over electron and hole components) plotted on top of the on-site potential as a function of the ladder index, where darker color corresponds to larger magnitude. The left, middle, and right panels are for Majoranas at  $0$ ,  $-\omega_1/2$  and  $-\omega_2/2$  energies, respectively. The other parameters are  $\omega_1 = 3.9$ ,  $\omega_2 = \omega_1 \times (\sqrt{5} + 1)/2$ ,  $J = 2$ ,  $\mu = 3.4$ ,  $\Delta = 0.2$ , and  $\Delta' = 0.15$ .

for a horizontal hopping, or

$$h_{0,1} = -\frac{i\Delta'}{2} \begin{pmatrix} 0 & \tau_- & & & & \\ -\tau_- & 0 & \tau_- & & & \\ & -\tau_- & \ddots & \ddots & & \\ & & \ddots & 0 & \tau_- & \\ & & & -\tau_- & 0 & \end{pmatrix} \quad (17)$$

for a vertical hopping.

In Fig. 8, we numerically calculate the Majorana wave function  $\phi_l(j) = (\phi_{l,e}(j), \phi_{l,h}(j))$  ( $l$  is the ladder index) at quasienergies  $0$ ,  $-\omega_1/2$ , and  $-\omega_2/2$  in a Kitaev chain of  $N = 100$  sites. We take 30 rungs of the quasiperiodic ladder in our numerical simulation. We see that both Majoranas are perfectly localized in both physical space and the quasiperiodic ladder.

Indeed, combining the two localization mechanisms, i.e., the Wannier-Stark localization and quasiperiodic localization, time-quasiperiodic Majoranas can be localized in the synthetic dimensions as discussed in the main text.

## SIGNATURES OF MAJORANA MULTIPLEXING IN CORRELATION FUNCTIONS

### Majorana operators in second quantization

Before analyzing signature of Majorana multiplexing, it is helpful to first introduce Majorana operators in second-quantization. Let  $|\Psi_\alpha(t)\rangle = \exp(-i\epsilon_\alpha t) |\Phi_\alpha(t)\rangle$  be a solution to the time-dependent Schrödinger equation

$$i\partial_t |\Psi_\alpha(t)\rangle = H(t) |\Psi_\alpha(t)\rangle, \quad (18)$$

where  $H(t)$  and  $|\Phi_\alpha(t)\rangle$  are time-quasiperiodic with the same frequencies, and  $\epsilon_\alpha$  is the quasienergy. Creation (annihilation) operators  $\psi_\alpha^\dagger(t)$  ( $\psi_\alpha(t) = (\psi_\alpha^\dagger(t))^\dagger$ ) corresponding to  $|\Psi_\alpha(t)\rangle$  can be defined as

$$\psi_\alpha^\dagger(t) = \sum_j C_j^\dagger \langle j | \Psi_\alpha(t) \rangle, \quad (19)$$

where  $j$  is the real space index,  $C_j^\dagger$  is the creation operator (may have multicomponents) at position  $j$  and  $\langle j | \Psi_\alpha(t) \rangle$  is the real space wave function (with the same number of components as in  $C_j$ ) of  $|\Psi_\alpha(t)\rangle$ .

In the case of time-quasiperiodic Kitaev chain, we have

$$\psi_\alpha(t) = e^{-i\epsilon_\alpha t} \sum_{j=1}^N \left[ c_j^\dagger \phi_{\alpha,e}(j,t) + c_j \phi_{\alpha,h}(j,t) \right], \quad (20)$$

where  $\phi_{\alpha,e}(j,t)$  and  $\phi_{\alpha,h}(j,t)$  are the two components in the Nambu wave function  $\langle j | \phi_\alpha(t) \rangle = (\phi_{\alpha,e}(j,t), \phi_{\alpha,h}(j,t))$ . Due to time-quasiperiodicity, we have

$$\phi_{\alpha,e/h}(j,t) = \sum_{\mathbf{m}} \exp(-i\mathbf{m} \cdot \boldsymbol{\omega}) \phi_{\mathbf{m},e/h}^\alpha(j), \quad (21)$$

where  $\phi_{\alpha,\mathbf{m},e/h}(j)$  are the solution of Eq. (1) in the main text represented in both real space and the synthetic lattice. For Majorana operators, in particular, we have  $\psi_\alpha(t) = \psi_\alpha^\dagger(t)$  for all  $t$ . This restricts the quasienergy to be  $\mathbf{n} \cdot \boldsymbol{\omega}/2$ . The wave function at quasienergy  $\epsilon_{\mathbf{n}} = \mathbf{n} \cdot \boldsymbol{\omega}/2$  is also restricted to satisfy  $\phi_{\mathbf{m},h} = \phi_{-(\mathbf{m}+\mathbf{n}),e}^*$ .

When there are two frequencies  $\omega_1$  and  $\omega_2$ , the Majorana operators of the chain at quasienergies 0,  $\omega_1/2$  and  $\omega_2/2$  can be written as

$$\psi_0^\dagger(t) = \sum_{j=1}^N \sum_{n,m} e^{-i(n\omega_1+m\omega_2)t} \left[ \phi_{n,m,e}(j) c_j^\dagger + \phi_{n,m,h}(j) c_j \right] \simeq \sum_{j=1}^N \left[ \phi_{0,0,e}(j) c_j^\dagger + \phi_{0,0,h}(j) c_j \right], \quad (22)$$

$$\psi_1^\dagger(t) = \sum_{j=1}^N \sum_{n,m} e^{-i(n\omega_1+m\omega_2)t} \left[ e^{i\omega_1 t/2} \phi_{n-1,m,e}(j) c_j^\dagger + e^{-i\omega_1 t/2} \phi_{n,m,h}(j) c_j \right] \quad (23)$$

$$\simeq \sum_{j=1}^N \left[ e^{i\omega_1 t/2} \phi_{-1,0,e}(j) c_j^\dagger + e^{-i\omega_1 t/2} \phi_{0,0,h}(j) c_j \right], \quad (24)$$

and

$$\psi_2^\dagger(t) = \sum_{j=1}^N \sum_{n,m} e^{-i(n\omega_1+m\omega_2)t} \left[ e^{i\omega_2 t/2} \phi_{n,m,e}(j) c_j^\dagger + e^{-i\omega_2 t/2} \phi_{n,m-1,h}(j) c_j \right] \quad (25)$$

$$\simeq \sum_{j=1}^N \left[ e^{i\omega_2 t/2} \phi_{0,-1,e}(j) c_j^\dagger + e^{-i\omega_2 t/2} \phi_{0,0,h}(j) c_j \right] \quad (26)$$

respectively. For Majoranas localized near the first site of the chain, the functions  $\phi_{n,m,e/h}(j)$  appeared in the above expressions decays exponentially as  $j$  increases.

### Correlation function

The presense of Majoranas of different types at the end of a time-quasiperiodic Kitaev chain can be detected using correlation functions of some local operators, such as the single particle Green's function. To be concrete, let us consider  $\langle 0 | \gamma_1(t) \gamma_1(0) | 0 \rangle$  where  $\gamma_1 = (c_1 + c_1^\dagger)/\sqrt{2}$ , and  $|0\rangle$  represents the BCS vacuum at  $t=0$ . The existence of Majoranas localized around the first site enables us to write

$$\gamma_1(t) = c_0 \psi_0(t) + c_1 \psi_1(t) + c_2 \psi_2(t) + \dots, \quad (27)$$

where  $\dots$  includes other extended state which has less contribution compared to the Majoranas. Hence, we have  $\langle 0 | \gamma_1(t) \gamma_1(0) | 0 \rangle$  will oscillate at frequencies  $\omega_1/2$  and  $\omega_2/2$ .

### Temporal disorder

To explore the robustness of these Majoranas in the presense of temporal disorder, we consider exponential correlated Gaussian noise in the drive. We replace  $\omega_i t$  by  $\omega_i t + \delta_i(t)$  with

$$\langle \delta_i(t) \delta_j(t') \rangle = \delta_{ij} \sigma^2 \exp(-|t-t'|/\tau_d), \quad (28)$$

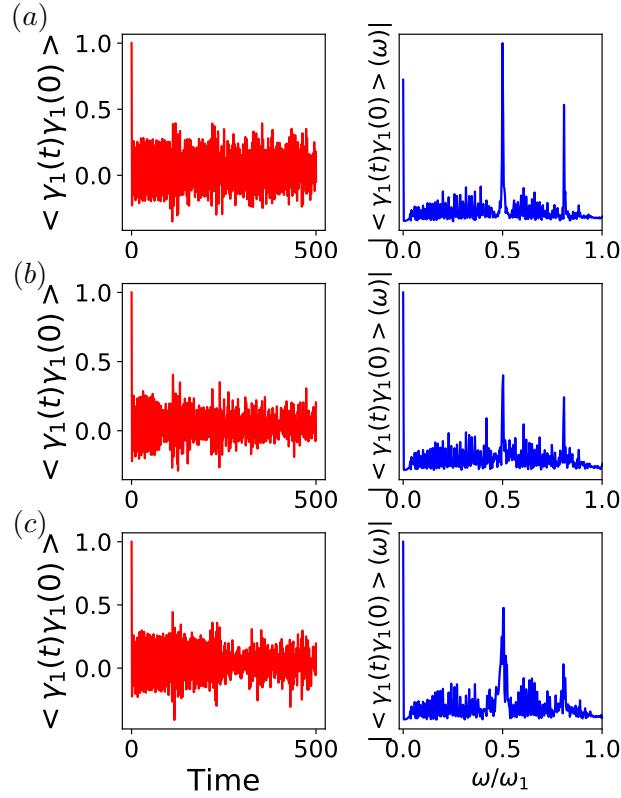


Figure 9.

Time evolution of  $\langle \gamma_1(t)\gamma_1(0) \rangle$  (left panels) and its Fourier transform in the frequency domain (right panels), simulated on the time-quasiperiodic Kitaev chain, with additional correlated Gaussian noise defined in Eq. (28). The other parameters are the same as in Fig. 4 of the main text. The parameters for the noise are  $\sigma = 0.1$ ; (a)  $\omega_2\tau_d = 1$ , (b)  $\omega_2\tau_d = 20$ , and (c)  $\omega_2\tau_d = 100$ .

where  $\tau_d$  is the correlation time, and  $\delta_i(t)$  is a Gaussian distributed random variable with zero mean and variance  $\sigma$ .

In Fig. 9, we show two numerical simulations of  $\langle \gamma_1(t)\gamma_1(0) \rangle$  using the same parameters as the ones in the main text, with additional correlated Gaussian noise. We see that peaks at  $0$ ,  $\omega_1/2$  and  $\omega_2/2$  are robust against moderate disorder strength  $\sigma$ , and correlation time  $\tau_d$ . As  $\tau_d$  gets longer, these peaks get broader.

### Commensurate frequencies

Practically, the two frequencies  $\omega_1$  and  $\omega_2$  can hardly be mutually irrational. Let us assume  $\omega_2/\omega_1 = p/q$ , with  $p, q \in \mathbb{Z}$ . In the synthetic space, the system is still Wannier-Stark localized along the electric field, while perpendicular to the field it becomes periodic, with a large unit cell when  $p$  and  $q$  are large. In this case, the wave functions are still localized within the unit cell due to the large variation of on-site energies between different sites. We still have Majoranas from pairing within the same site or between neighboring sites.

Let approximate the golden ratio  $(\sqrt{2} + 1)/2$  by  $5/3$ , and take  $\omega_2/\omega_1 = 5/3$  for the time-dependent Kitaev chain. Fig. 10 shows the wave function of the Majoranas in synthetic space and in real space. We find that the Majorana amplitudes are only localized with unit cells perpendicular to the direction of the electric field. In Fig. 11, we show the correlation  $\langle \gamma_1(t)\gamma_1(0) \rangle$ , and also find peaks at  $\omega_1/2$  and  $\omega_2/2$ .

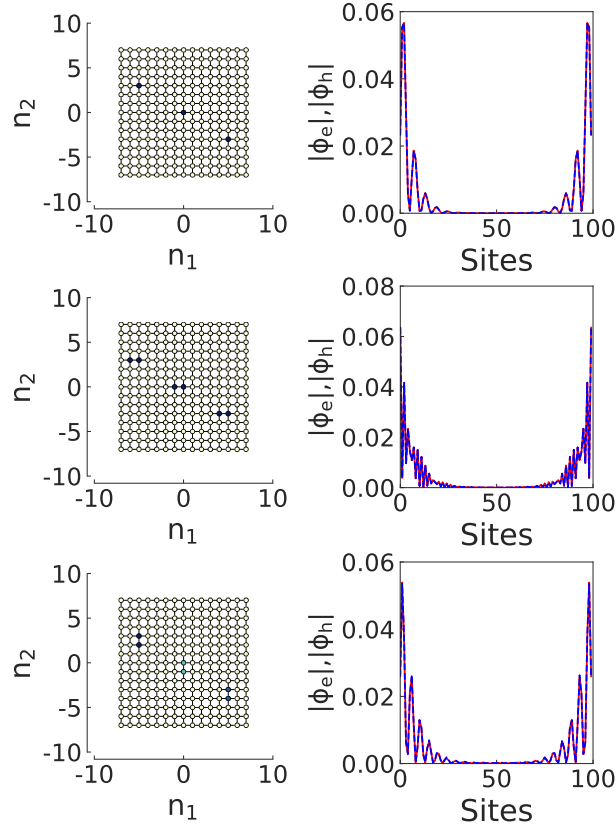


Figure 10. Numerical solution of the 0-frequency and time-quasiperiodic Majorana states on the 2D synthetic lattice of size  $15 \times 15$ . Each site of the lattice corresponding to a Kitaev chain of length  $N = 100$ . Left:  $|\phi_{n_1, n_2}|^2$  for the  $0$ ,  $\frac{\omega_1}{2}$ , and  $\frac{\omega_2}{2}$  Majoranas on the 2D synthetic lattice, where the darker color corresponds to a larger magnitude. Right: the absolute value of the corresponding Majorana wave function, summed over the 2D synthetic lattice. The electron and hole components  $\phi_e, \phi_h$  are plotted as red solid and blue dashed curves. The other parameters are  $\omega_1 = 3.9$ ,  $\omega_2/\omega_1 = 5/3$ ,  $J = 2$ ,  $\mu = 3.4$ ,  $\Delta = 0.2$ , and  $\Delta' = 0.15$ .

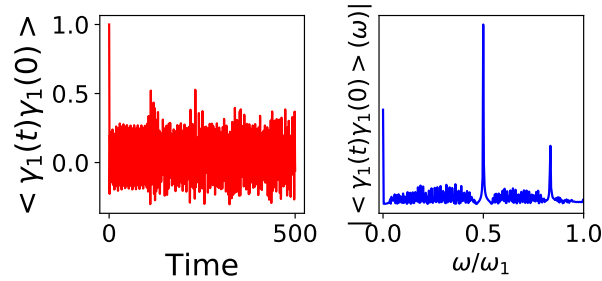


Figure 11. Time evolution of  $\langle \gamma_1(t) \gamma_1(0) \rangle$  (left panels) and its Fourier transform in the frequency domain (right panels), with  $\omega_1 = 3.9$ ,  $\omega_2/\omega_1 = 5/3$ ,  $J = 2$ ,  $\mu = 3.4$ ,  $\Delta = 0.2$ , and  $\Delta' = 0.15$ .